ChemComm

Accepted Manuscript

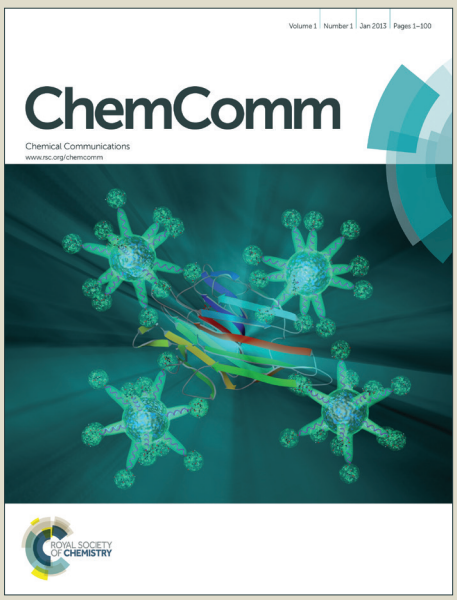

ROYAL SOCIETY OF CHEMISTRY

www.rsc.org/chemcomm

ARTICLE TYPE www. rsc.org/xxxxxx | XXXXXXXX

Influence of Moisture on the Preparation, Crystal Structure, and Photophysical Properties of Organohalide Perovskites†

Kelsey K. Bass,[a] R. Eric McAnally,[a] Shiliang Zhou,[a] Peter I. Djurovich,[a] Mark E. Thompson,[a] Brent C. Melot[a]*

Received Xth XXXXXXXXXX 20XX, Accepted Xth XXXXXXXXX 20XX
First published on the web Xth XXXXXXXXXX 200X
DOI: 10.1039/b000000x

The effect of preparing lead-based organohalide perovskites under inert conditions has been investigated. We find that when prepared under anhydrous conditions, only poorly crystalline powders were obtained. On exposure to small amounts of moisture a rapid crystallization into the expected cubic unit cell for $CH_3NH_3PbBr_3$ and tetragonal cell for $CH_3NH_3PbI_3$ is observed. While the as-prepared iodide phase is non-emissive, the lifetime of the emission for the bromide is found to be much longer when prepared under atmospheric conditions.

Organo-halide perovskites have attracted considerable attention for their use in solution processable solar cells with power conversion efficiencies of over 15%.[1–19] Most reports have focused on improving device performance whereas the fundamental nature of the perovskite phases used in the devices is less explored. While it has been acknowledged that devices should be prepared in conditions with less than 1% humidity,[11] few reports have been made on the influence of the atmosphere on the resulting product. Niu *et al.* performed experiments to compare the structure and performance of $CH_3NH_3PbI_3$ photovoltaic devices before and after exposure to 60% humidity, but prepared all of their samples in ambient conditions.[20] To better understand the role of moisture in the preparation of these phases, we have synthesized $CH_3NH_3PbBr_3$ and $CH_3NH_3PbI_3$ in an air free environment and studied the structure and photophysical properties of the air free and air exposed powders and films.

All reagents were purchased fresh from the respective supplier and kept inside an Ar-filled glove box with less than 0.1 ppm of moisture and approximately 0.30 ppm of oxygen. CH_3NH_3Br and CH_3NH_3I were prepared by mixing 40% CH_3NH_2 in water (Spectrum Chemical Mfg. Corp.) with concentrated HBr (Sigma Aldrich, 48%) or HI (Sigma Aldrich, 57%) as described previously.[21] Prior to use, CH_3NH_3I was purified further by sublimation to remove a yellow-orange coloration that was likely the result of I_2 present in the HI. Powdered reagents like $Pb(NO_3)_2$ (Acros Organic), CH_3NH_3Br, and CH_3NH_3I were weighed and sealed inside of the glove box before moving to a Schlenk line for the reaction. Ground glass fittings were preferred over rubber septa due to the reactivity of the septa with the fumes of the concentrated acids. A typical synthesis was performed under a constant positive pressure of nitrogen with stoichiometric amounts of $Pb(NO_3)_2$ and CH_3NH_3X in concentrated HX. The solution was heated to 100°C until the powders were fully dissolved before cooling to room temperature. The resulting orange (bromide) and black (iodide) mixture of crystals and powder were washed with anhydrous diethyl ether and dried under vacuum. We note that slower cooling from the reaction temperature does not produce crystalline powders but results in larger, poorly crystalline particles that crystallize at a slower rate when exposed to moisture.

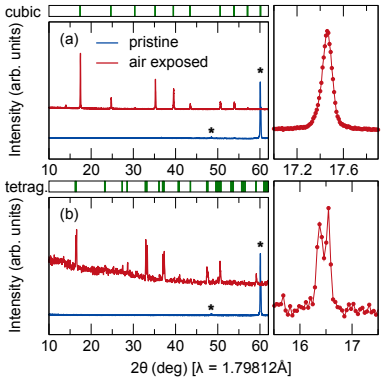

Fig. 1 Comparison of laboratory powder diffraction data for (a) $CH_3NH_3PbBr_3$ and (b) $CH_3NH_3PbI_3$ materials prepared/characterized under inert atmosphere (blue line) and exposed to ambient atmosphere (red lines). The panels on the right emphasize the lowest angle peak which splits on distortion from the cubic to tetragonal phase. The asterisks denote reflections from the Be window of the air-free XRD cell.

Fig. 1 shows X-ray diffraction patterns collected on a

† Electronic Supplementary Information (ESI) available: [details of any supplementary information available should be included here]. See DOI: 10.1039/b000000x/

[a] *Department of Chemistry, University of Southern California, Los Angeles, CA 90089 E-mail: melot@usc.edu*

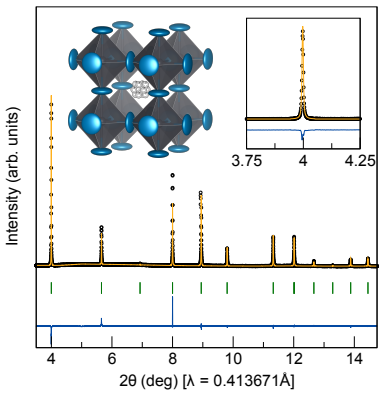

Fig. 2 Results from the Rietveld refinement of the cubic structure of $CH_3NH_3PbBr_3$ at room temperature against high resolution synchrotron diffraction data obtained from the 11-BM beam line at Argonne National Laboratory on powders which were exposed to the atmosphere. R_{Bragg} =7.48%, R_f =3.19%, χ^2 =1.38. The inset on the left illustrates the resulting structure with atoms visualized at the 95% probability level. The inset on the right emphasizes the 100 Bragg reflection of the cubic perovskite.

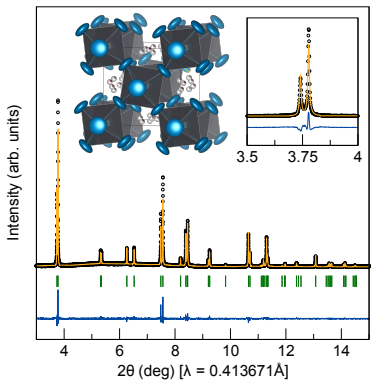

Fig. 3 Rietveld refinement of the tetragonal structure of $CH_3NH_3PbI_3$ at room temperature against 11-BM data for powders which were exposed to the atmosphere. R_{Bragg} =5.23%, R_f =5.39%, χ^2 =1.09. The inset on the left illustrates the resulting structure with atoms visualized at the 95% probability level. The inset on the right emphasizes the splitting of the 100 peak into the 002 and 110 planes of the tetragonal structure.

Bruker D8 powder diffractometer equipped with a Lynxeye detector and Co-Kα tube. The pristine patterns were collected using an air-tight stainless steel cell equipped with a 25 mm Be window that has been described previously.[22] Very weak reflections are seen in the powders prior to exposure to atmosphere for either the $CH_3NH_3PbBr_3$ [Fig. 1 (a)] or the $CH_3NH_3PbI_3$ [Fig. 1 (b)] powders. On opening the cell and allowing to sit on the bench top for only a few minutes, peaks which could be indexed to a cubic unit cell were found for the bromide and a tetragonal cell for the iodide. The difference in quality of the patterns is because the iodide had to be scanned at a much faster rate. Allowing the black powder to sit for more than a few minutes in air resulted in the powder taking on a brown tint, indicating a small conversion to the yellow hydrated phase. No diffraction peaks were seen for the hydrated phase, however, so the reaction likely occurred primarily on the surface without much penetration into the bulk.

To mitigate the conversion to the hydrated phase and obtain a more accurate picture of the structure, the as-prepared powders were briefly exposed to ambient atmosphere before sealing in kapton capillaries and sent for synchrotron diffraction experiments at the 11-BM beam line at Argonne national lab. The results of the Rietveld refinement of $CH_3NH_3PbBr_3$ and $CH_3NH_3PbI_3$ structures against the synchrotron data are shown in Figs 2 and 3 respectively. The high intensity and resolution of the 11-BM data shows extremely phase-pure powders with no sign of any secondary phases. Anisotropic atomic displacement parameters were refined for both phases and show a significant degree of disorder in the halide ions. This is probably related to rotational disorder associated with the methylammonia groups which are known to be highly disordered at room temperature.[3,23,24] The tetragonal distortion in the iodide is attributed to a slight ordering of these groups, and results in an alternating 16° rotation of the corner-sharing octahedra down the length of the *c* axis of the unit cell which generates new reflections at 6.3° and 6.5° in 2θ. There is simultaneously a compression of the *c/a* ratio from the ideal 1.50 to 1.43 which splits the [100] Bragg reflection as emphasized in the inset.

To distinguish the effect of oxygen from atmospheric moisture, dry O_2 and moist N_2 were separately passed over a small amount of the pristine bromide powder. Importantly, exposure to the anhydrous gases had absolutely no effect on the observed diffraction patterns, while the moist nitrogen was found to rapidly trigger the crystallization into the cubic phase. It is not immediately clear how moisture promotes this rapid crystallization. However, considering these organohalide perovskites are extremely soluble in aqueous solutions, it is possible that humidity in the air triggers nucleation and crystallization as has been seen in amorphous lactose particles.[25,26] Similar effects also occur with organic solvents inducing crystallization of $Na_3Au(SO_3)_2$ and tris(8-hydroxyquinoline)aluminum films.[27,28]

Since the as-prepared powders are non-emissive, the role of moisture on the photophysical properties was explored by dissolving powders which had never been exposed to moisture in anhydrous DMF at a concentration of 10 wt%. Two sets of films were then cast; one inside an Ar-filled glove box (less than 0.01 ppm of moisture and 23.5°C) and the other in open air (58.2% humidity and 22.6°C). X-ray diffraction patterns confirmed that films cast under anhydrous con-

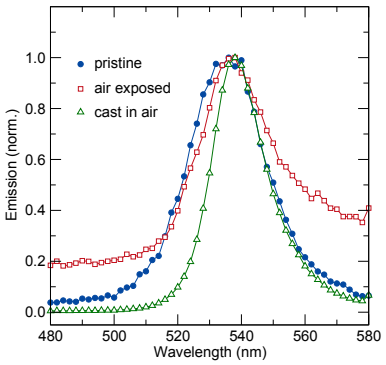

Fig. 4 Optical emission spectra for pristine films of $CH_3NH_3PbBr_3$ before (filled blue circles) and after exposure to atmosphere (unfilled red squares) as well as those cast in air (unfilled green triangles).

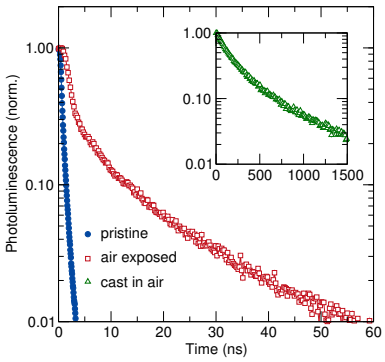

Fig. 5 Time-resolved photoluminescence emission spectra for pristine films (filled blue circles) and films which were exposed to ambient atmosphere (unfilled red squares) for the $CH_3NH_3PbBr_3$. Note the exceptionally longer lifetimes when exposed to air and recall that all iodide-based phases failed to show any sign of luminescence.

ditions remained poorly crystalline and that exposure to moisture resulted in rapid crystallization to highly oriented crystallites which predominantly showed diffraction peaks associated with [00l] Bragg planes much like in the films cast in air. Analysis using scanning electron microscopy demonstrated that the morphology of the films cast under Ar versus those cast in air is different. The films cast in air exhibit smaller particle sizes, which is counter-intuitive to the enhanced photoluminescence lifetime. Thus, particle size is irrelevant in these films and does not explain the differences in lifetimes. The higher crystallinity of the particles in the films cast in air seems to allow the films to exhibit increased lifetimes. We note that similar problems with obtaining complete wetting of the substrate were encountered as previously reported,[29] but additives to improve coverage were avoided to reduce any potential impact on the performance.

In order to confirm that there were no major differences between the poorly crystalline and crystalline phases, the optical emission spectra for both phases were collected. Aside from a slight difference in peak width, all three films were confirmed to display emission at the previously reported wavelength of 540 nm for the bromide phase (Fig. 4), albeit with very low efficiency ($\Phi < 0.01$). In contrast, no emission was observed from films prepared from the iodide powders around the expected wavelength of 770 nm. Very weak emission was observed for the iodide closer to 520 nm, but this is believed to be associated with a small impurity related to the yellow hydrated form. This observation is in keeping with what has previously been reported for materials prepared using solution deposition techniques.[30]

Time-resolved emission data were recorded using a time-correlated single photon counting (TCSPC) technique. Fig. 5 shows the resulting transient decays for a film cast in air-free conditions, the same film which was then exposed to the atmosphere, and the one cast in air. The difference between films cast in air and under inert atmosphere is striking. Films exposed to air or cast in atmospheric conditions were found to show increasingly long luminescent lifetimes. Given that there are no substantial morphological differences between the films, this result is likely a result of differences in the crystallinity of each film. The pristine films are poorly crystalline and show the most rapid decay in the emission lifetime. It is not surprising that only after the films are crystalline that emission life times begin to reflect what has been reported in the literature.[29,31] The loss of long-range periodicity in the poorly crystalline films appears to provide new routes by which the excited state can decay at a significantly accelerated rate. Our results then appear to indicate that the presence of a small amount of moisture is absolutely necessary in order to produce the highly crystalline films which exhibit the long-lived excited states that have been seen in the literature, although it is still not exactly clear how moisture promotes crystallization.

In summary, our results demonstrate that the synthetic conditions under which organohalide perovskites are prepared plays a critical role in promoting crystallization. Further studies are needed to understand why exposure to moisture triggers the crystallization of the perovskite phase, but it is clear from the photoluminescence data that the excited state in the amorphous films is quenched at a significantly faster rate than those which were fully crystallized.

References

1 K. Liang, D. B. Mitzi and M. T. Prikas, *Chemistry of Materials*, 1998, **10**, 403–411.
2 C. R. Kagan, D. B. Mitzi and C. D. Dimitrakopoulos, *Science*, 1999, **286**, 945–947.
3 Y. Kawamura, H. Mashiyama and K. Hasebe, *Journal of the Physical Society of Japan*, 2002, **71**, 1694–1697.

4 A. Kojima, K. Teshima, Y. Shirai and T. Miyasaka, *Journal of the American Chemical Society*, 2009, **131**, 6050–6051.

5 J.-H. Im, C.-R. Lee, J.-W. Lee, S.-W. Park and N.-G. Park, *Nanoscale*, 2011, **3**, 4088–4093.

6 L. Etgar, P. Gao, Z. Xue, Q. Peng, A. K. Chandiran, B. Liu, M. K. Nazeeruddin and M. Grtzel, *Journal of the American Chemical Society*, 2012, **134**, 17396–17399.

7 Z. M. Beiley and M. D. McGehee, *Energy Environ. Sci.*, 2012, **5**, 9173–9179.

8 M. M. Lee, J. Teuscher, T. Miyasaka, T. N. Murakami and H. J. Snaith, *Science*, 2012, **338**, 643–647.

9 H.-S. Kim, C.-R. Lee, J.-H. Im, K.-B. Lee, T. Moehl, A. Marchioro, S.-J. Moon, R. Humphry-Baker, J.-H. Yum, J. E. Moser, M. Grätzel and N.-G. Park, *Scientific Reports*, 2012, **2**, 1–7.

10 I. Chung, B. Lee, J. He, R. P. H. Chang and M. G. Kanatzidis, *Nature*, 2012, **485**, 486–489.

11 T. Baikie, Y. Fang, J. M. Kadro, M. Schreyer, F. Wei, S. G. Mhaisalkar, M. Graetzel and T. J. White, *J. Mater. Chem. A*, 2013, **1**, 5628–5641.

12 J. M. Ball, M. M. Lee, A. Hey and H. J. Snaith, *Energy Environ. Sci.*, 2013, **6**, 1739–1743.

13 J. Burschka, N. Pellet, S.-J. Moon, R. Humphry-Baker, P. Gao, M. K. Nazeeruddin and M. Grätzel, *Nature*, 2013, **499**, 316–319.

14 M. Liu, M. B. Johnston and H. J. Snaith, *Nature*, 2013, **501**, 395–398.

15 N.-G. Park, *The Journal of Physical Chemistry Letters*, 2013, **4**, 2423–2429.

16 S. D. Stranks, G. E. Eperon, G. Grancini, C. Menelaou, M. J. P. Alcocer, T. Leijtens, L. M. Herz, A. Petrozza and H. J. Snaith, *Science*, 2013, **342**, 341–344.

17 G. Xing, N. Mathews, S. Sun, S. S. Lim, Y. M. Lam, M. Grtzel, S. Mhaisalkar and T. C. Sum, *Science*, 2013, **342**, 344–347.

18 G. E. Eperon, V. M. Burlakov, P. Docampo, A. Goriely and H. J. Snaith, *Adv. Funct. Mater.*, 2014, **24**, 151–157.

19 S. Sun, T. Salim, N. Mathews, M. Duchamp, C. Boothroyd, G. Xing, T. C. Sum and Y. M. Lam, *Energy Environ. Sci.*, 2014, **7**, 399–407.

20 G. Niu, W. Li, F. Meng, L. Wang, H. Dong and Y. Qiu, *J. Mater. Chem. A*, 2014, **2**, 705–710.

21 M. J. Carnie, C. Charbonneau, M. L. Davies, J. Troughton, T. M. Watson, K. Wojciechowski, H. Snaith and D. A. Worsley, *Chem. Commun.*, 2013, **49**, 7893–7895.

22 J. B. Leriche, S. Hamelet, J. Shu, M. Morcrette, C. Masquelier, G. Ouvrard, M. Zerrouki, P. Soudan, S. Belin, E. Elkam and F. Baudelet, *Journal of The Electrochemical Society*, 2010, **157**, A606–A610.

23 H. Mashiyama and Y. Kurihara, *Journal of the Korean Physical Society*, 1998, **32**, S156–S158.

24 C. Quarti, G. Grancini, E. Mosconi, P. Bruno, J. M. Ball, M. M. Lee, H. J. Snaith, A. Petrozza and F. D. Angelis, *The Journal of Physical Chemistry Letters*, 2014, **5**, 279–284.

25 D. Burnett, F. Thielmann, T. Sokoloski and J. Brum, *International Journal of Pharmaceutics*, 2006, **313**, 23 – 28.

26 D. Mahlin, J. Berggren, G. Alderborn and S. Engstrm, *Journal of Pharmaceutical Sciences*, 2004, **93**, 29–37.

27 X. Sun and M. Hagner, *Chemistry of Materials*, 2008, **20**, 2869–2871.

28 D. J. Mascaro and V. Bulovic, *JCIS - Proceedings*, 2009, **3**, 1441–1444.

29 G. E. Eperon, S. D. Stranks, C. Menelaou, M. B. Johnston, L. M. Herz and H. J. Snaith, *Energy Environ. Sci.*, 2014, **7**, 982–988.

30 C. C. Stoumpos, C. D. Malliakas and M. G. Kanatzidis, *Inorganic Chemistry*, 2013, **52**, 9019–9038.

31 N. Pellet, P. Gao, G. Gregori, T.-Y. Yang, M. K. Nazeeruddin, J. Maier and M. Grätzel, *Angewandte Chemie International Edition*, 2014, **53**, 3151–3157.